Enhancement of Antibacterial and Mechanical Features of Glass Ionomer Restoration by Adding ZnO Nanoparticles Prepared by PLAL: In Vitro Study

Ghufran. S. Jaber
Division of Laser science and technology, Department of Applied Science, University of Technology - Iraq;

khawla khashan (khawla_salah@yahoo.com)
Division of Laser science and technology, Department of Applied Science, University of Technology - Iraq; https://orcid.org/0000-0001-9028-9191

Maha Jamal Abbas
College of Dentistry, Al-Mustansiriyah University

Research Article

Keywords: Laser ablation in liquid, Glass ionomer restoration, Zinc oxide nanoparticles, Streptococcus mutant and Compressive strength

Posted Date: March 8th, 2021

DOI: https://doi.org/10.21203/rs.3.rs-284225/v1

Abstract

The objective of this manuscript was to study the antibacterial and mechanical effect on composition ZnONPs-Glass Ionomer restoration. Zinc oxide nanoparticles prepared by laser ablation in liquid at different concentrations. After that, the glass ionomer was adding in calculated amount to get homogenous composition. The physical properties of resulted NPs were examined by FTIR, XRD, TEM, and AFM. The Antibacterial activity against *streptococcus mutant* and compressive strength were also measured. The result of the FTIR spectrum confirms the formation of the Zn-O bond. XRD pattern shows peaks at 28..55°, 31.21° and 42.70°, correspond to the (100) (101) and (102) crystal planes of cubic Zinc Oxide structure. TEM image exhibits spherical and homogenous ZnO nanoparticles with particle size <50nm. Also, the result shows a significant increase in the antibacterial property of ZnO-GI with good modifying the mechanical properties. Thus adding ZnO nanoparticles to glass ionomer restoration can be considered as a better alternative to conventional GI.

1. Introduction

Secondary caries is a problem that occurs in the mouth within restoration that leads to fall of the restorative materials. One of the main causes of secondary caries was Oral Streptococcus mutans (SM) which cause dental plaque biofilm formation. So that, increase the tooth's reluctance to secondary decay an appropriate restorative material is used for prevention of dental caries by stop bacterial growth [1-3]. Glass ionomer popular restorative dental material based on acid base reaction [4,5]. It has wide dental applications as restoration of primary teeth, GI regarded a good chemical adhesion with tooth, low thermal expansion near to the tooth coefficient and has ability to fluoride release Therefore, and it is considered an anti-bacterial with high efficiency [6-9]. In spite of the good features, GI high porosity with large internal cracks leading to weak mechanical properties that leading to form a secondary caries [10]. The adding nanoparticles which, in turn, are characterized by small particle size and large surface area [11] these properties allow a harmonious interaction with the micro cracks of GI-surface [12]. Zinc oxide nanoparticles good choice with GI because, was used as an antibacterial agent and incorporated in many dental products [13]. Zinc oxide Nanoparticles (ZnO-NPs) is a biocompatible material, non-toxic to human cells but more toxic to the bacteria. ZnO-NPs can inhibit the growth of oral SM and plaque formation [14-15]. Also, the antibacterial effect of ZnO-NPs increase by increase of the concentration and decrease in nanoparticles size[16]. Many techniques is used to fabricated nanoparticles for example: chemical and physical vapor deposition, sol-gel, and flame synthesis .These methods were complex setup and need special parameters such as temperature and pressure to get the desired composition and size distribution. Now days, laser ablation of materials was nearly new technique first invented at 1993 by Fojtik et al has proven merits as the common efficient procedure for get nanoparticles [17-19]. This is the chosen method is characterized by its ease, efficiency and does not require complicated situations or specific conditions to obtain a nanoscale solution [20]. At this promising method can control on size and concentration of fabricated ZnO nanomaterial via change the laser parameters. The study revolves

around comparing and evaluates the mechanical and antibacterial activity of enhanced conventional glass ionomer restoration with ZnONPs.

2. Materials And Method

2.1 Preparation of ZnONPs –GI Composition

ZnO nanoparticles synthesis by pulse laser ablation in liquid, first the zinc bulk immersed in 1ml of double distilled water at room temperature. The Nd:Yag (Q-switched pulsed) with (1064 nm,1Hz) laser energy 600 mJ to prepare ZnONPs. Laser beam focused with focal length =20cm of lens at distance =5cm about the target, figure (1). The glass container was rotated for prevent etching and get homogenous nanoparticles [21]. The samples divided into three groups ZnONPs (100,150 and 200) pulses and fixed the laser energy. After that the glass ionomer(Riva, Australia) was mixed with P/L ratio 1:0.5:0.5 (one scoop powder and 0.5 drop of liquid+0.5 drop of ZnONPs). In order to obtain three groups with different concentration of zinc oxide nanoparticles changing laser pulses to (100,150 and 200) and fixed laser energy then adding to constant amount of glass ionomer.

2.2 Antibacterial enhancement

The 1.9 gram of mueller hinton agar was dissolving in 50 mL of DDW then, shaking, heating and sterilization through autoclaving for 15 minute at temperature of 121° C and pressure of 15 lbs. After that cooled and divided on the petri-disk until be sold layer. Streptococcus mutans was sweep all the surface of petri-dish from all direction. The well making by using the tip of micropipette with 6mm diameter, ZnONPs samples and enhanced samples colloidal with 50µL filled the well. Then leaving the agars for 48h in incubation finally, inhibition zone diameter of the all samples antibacterial effect was calculated.

2.3 Tooth Preparation

Three fresh, free caries, for 20-35 years old patients and third premolars teeth extracted from dental clinic (Dr. Wissam, in Al-Harithiya). Teeth washed with de-ionized water, and then each tooth was wiped with acetone to remove any debris then stored with 50 ml of normal saline. Buckle surfaces of each tooth were coated with red nail varnish leaving circular hole with dimensions (4 * 4) mm. After that, the composition of enhance GI-restoration was filled the tooth, see figure2

2.4 Mechanical enhancement

The compressive strength was measured by using the Universal testing machine (England). The tooth specimens placed between the plates of the universal testing machine fixed on enhanced restoration sides. A compressive load with maximum force applied on tooth samples until the specimen fractured. The compressive strength of the samples was measured after 48 h in normal saline.

3. Result And Discussion

3.1 FTIR Analysis

Fourier transformer infrared technique was used to identify the chemical bonding and component of substance. The spectrum peak of the ZnONPs was prepared by laser ablation in liquid listed in figure 3(A). The fundamental vibration mode was lie at (3000Cm^{-1}) this is due O-H stretching bond stretching and distortion respectively assigned to the water absorption on the metal surface. The peak at rang 1000-1800 cm^{-1} refer to C=O asymmetric stretching bond while an absorption at 400-800cm^{-1} refer to indicate coordination of ZnONPs stretching vibrations [22-23]. While figure (3B) exhibits FTIR results of ZnONPs-GI restoration peaks attributable to polyacrylic acid (PAA) at 1600 cm^{-1} (C=O stretch), Peak representing water component at 3000cm^{-1} (O-H stretch) was also obtained. These peaks were looked broader and shifted to 300 cm^{-1} after GI modification with ZnONPs. It may be attributed to the incorporation of ZnONPs to the active C=O group in GI. This suggestion is confirmed by the decrease in the transmission observed after adding GI, which could be explained by the formation of polyacrylate salts [24].

3.2 XRD Measurement

X-ray diffraction of ZnONPs was estimated at figure 4, were the diffraction peaks calculated at position 2θ (10–80°) with angles of 28..55°, 31.21° and 42.70°,correspond to the reflection from the (100) (101) and (102) crystal planes with cubic zinc oxide structure [19]. The particles size calculated by using Scherer equation: D=0.89λ/βCosθ, Where D of the particles size, λ is the wavelength of Cu Kα,, β is the full width at the half- maximum (FWHM) by using of the ZnONPs line and θ is the diffraction angle by using xpert high score plus program. [20]. Table 2 calculated the mean grain size and lattice strain of the ZnONPs. The Williamson-Hall (W-H) measurement used to calculated lattice strain (ε) of the ZnONPs between β cosθ against 4sinθ was straight line gives information about the strain in the form of the slope. The crystal perfect when all atoms are at rest on their correct lattice positions in the crystal structure [25]. The variation of the lattice strains in samples due the variation in (hk.l) with linear behavior is observed because of the small difference in the average particle size distribution [26].

3.3 TEM & Size distribution Image

Figure 5 shows the TEM images for ZnONPs colloidal prepared at energies 600 mJ, a size of particles varies with domain a range between few tens of nanometers. These photos detect that the nanoparticles produced due to the interaction of laser pulse with zinc target are roughly uniform the images of the different shapes of the synthesized ZnO NPs [27]. The morphology of the NPs showed hexagonal, spherical and rod-shaped structures with some agglomerated large and small particles. The size-distribution that indicates strong appearance of nanoparticle and aggregation at higher laser pulses according to the electrostatic attractive force between them, which fabricated because of electric double layer on the surface of nanoparticles[28].

3.4 Atomic Force Microscope Measurement

AFM images with three dimensions for zinc oxide colloidal and zinc oxide NPs- Glass ionomer restoration showed in figure 6. Larger number of laser pulses lead to a smaller particle size because of the longer ablation time leads to a narrowing of the nanoparticle size distribution due to the interaction of the ablating laser beam with the produced Nanoparticles [29,30] and The decrease in the particle size appear because of laser fragmentation effect. Since laser pulse causes larger particles to participate to smaller and smaller one. According to the AFM images ZnONPs-GI composition were smooth surface despite some small particles and grain clusters.

3.5 Antibacterial activity

Figure 7 shows the antibacterial activity of ZnONPs and ZnONPs-GI, the antibacterial activity of zinc oxide nanoparticles significantly increased with high concentration of nanoparticles. The ZnONPs synthesize by PLAL at fixed laser energy (600mJ) and different laser pulse number show higher antibacterial activity against streptococcus mutans bacterial strains [31]. The antibacterial action of ZnONPs work via releasing reactive oxygen species (ROS), then interacting with the bacteria wall by electrostatic forces leading loss of extracellular content and bacterial cell death [32]. Also, the result show in figure 6 a significant antibacterial activity of GI after incorporated with different concentration of ZnONPs samples in comparison to the empty wells and GI. This result was approve with (Hojati et al.) [33]. That by increasing the nanoparticles concentration the antibacterial activity increase.

3.6 Compressive Strength

The mean compressive strength of the control and experimental groups after 48- hours after preparation in vitro study, see figure 8. The storage of tooth samples in normal saline is shown in Table 2 statistically enhanced significant differences after adding the ZnONPs. The enhanced restoration strength increased by increase ZnONPs concentration that’s attributed to the increase in nanoparticles help to fill the micro cracking in surface layer of glass ionomer.

4. Conclusions

1- The incorporation ZnO-NPs into glass ionomer enhances its antibacterial activity against oral *Streptococcus mutans* and increase the compressive strength with increasing concentration of colloidal-ZnO.

2- The FTIR confirmed that, the interaction between the zinc oxide nanoparticles and glass ionomer was occurred through the C=O functional group of poly acrylic acid of glass ionomer.

3- Zinc oxide nanoparticles were formation with cubic structure detected by the X-ray diffraction and calculated the lattice strain takes linear behavior. The TEM image shows the homogenous distribution with almost spherical and other different shapes.

4- The main factors enhance the antibacterial activity of ZnONPs their decrease in particles size and increase concentration of suspension.

Declarations

due to technical limitations, Declarations section is not available for this version.

References

[1] T. M. Hamdy, “Application of Nanotechnology in Dental Caries Management,” *EC Dent. Sci.*, 161, 52–55, 2017

[2] G. Szozda, K. Nowakowska, and D. Pawluch, “Comparative evaluation of the antibacterial activity of nitrofuran derivatives,” *Pol. Tyg. Lek.*, 42, 967–969, 1987.

[3] A. Emamifar, M. Kadivar, M. Shahedi, and S. Soleimanian-Zad, “Effect of nanocomposite packaging containing Ag and ZnO on inactivation of Lactobacillus plantarum in orange juice,” *Food Control*, 22, 408–413, 2011, doi: 10.1016/j.foodcont.2010.09.011.

[4] S. Sidhu and J. Nicholson, “A Review of Glass-Ionomer Cements for Clinical Dentistry,” *J. Funct. Biomater.* 7, 16, 2016, doi: 10.3390/jfb7030016.

[5] S. Shaikh *et al.*, “Mechanistic insights into the antimicrobial actions of metallic nanoparticles and their implications for multidrug resistance,” *Int. J. Mol. Sci.*, 20, 1–15, 2019, doi: 10.3390/ijms20102468.

[6] R. Jones, *Bone*, 23, 1–7, 2014, doi: 10.1016/j.tibtech.2013.05.010.Nanotechnology-based.

[7] S. S. Sonia, L. J. K. H. Linda Jeeva Kumari, R. K. Ruckmani, and S. M. Sivakumar, “Antimicrobial and antioxidant potentials of biosynthesized colloidal zinc oxide nanoparticles for a fortified cold cream formulation: A potent nanocosmeceutical application,” *Mater. Sci. Eng. C*, 79, 2018

[8] J. Perrière *et al.*, “Comparison between ZnO films grown by femtosecond and nanosecond laser ablation,” *J. Appl. Phys.*, 91, 690–696, 2002, doi: 10.1063/1.1426250.

[9] E. Solati and D. Dorranian, “Estimation of Lattice Strain in ZnO Nanoparticles Produced by Laser Ablation at Different Temperatures,” *J. Appl. Spectrosc.*, 84, 490–497, 2017, doi: 10.1007/s10812-017-0497-0.

[10] A. Sirelkhatim *et al.*, “Review on zinc oxide nanoparticles: Antibacterial activity and toxicity mechanism,” *Nano-Micro Lett.*, 7, 219–242, 2015, doi: 10.1007/s40820-015-0040-x.

[11] B. A. Sevinç and L. Hanley, “Antibacterial activity of dental composites containing zinc oxide nanoparticles,” *J. Biomed. Mater. Res. - Part B Appl. Biomater.*, 94, 22–31, 2010, doi: 10.1002/jbm.b.31620.

[12] I. Kim, K. Viswanathan, G. Kasi, S. Thanakkasaranee, K. Sadeghi, and J. Seo, “ZnO Nanostructures in Active Antibacterial Food Packaging: Preparation Methods, Antimicrobial Mechanisms, Safety Issues,

Future Prospects, and Challenges," *Food Rev. Int.*, 00, 1–29, 2020, doi: 10.1080/87559129.2020.1737709.

[13] R. Krithiga and N. Selvi, "An X-Ray assessment of ZnO : Li and ZnO : K nano grains,"119, 3101–3109, 2018.

[14] R. Byun, M. A. Nadkarni, K. L. Chhour, F. E. Martin, N. A. Jacques, and N. Hunter, "Quantitative analysis of diverse Lactobacillus species present in advanced dental caries," *J. Clin. Microbiol.*, 42, 3128–3136, 2004, doi: 10.1128/JCM.42.7.3128-3136.2004.

[15] G. Sharmila *et al.*, "Biosynthesis, characterization, and antibacterial activity of zinc oxide nanoparticles derived from Bauhinia tomentosa leaf extract," *J. Nanostructure Chem.*, 8, 293–299, 2018, doi: 10.1007/s40097-018-0271-8.

[16] M. F. Khan *et al.*, "Sol-gel synthesis of thorn-like ZnO nanoparticles endorsing mechanical stirring effect and their antimicrobial activities: Potential role as nano-Antibiotics," *Sci. Rep.*, 6, 1–12, 2016, doi: 10.1038/srep27689.

[17] A. J. Ghazai, J. Aziz, and N. T. Yassen, "Effect of Laser Pulses and Energy on the Structural Properties of ZnO Thin Film Prepared Using PLA Technique," 1–10, 2017, doi: 10.20944/preprints201704.0017.v1.

[18] V. Mote, Y. Purushotham, and B. Dole, "Williamson-Hall analysis in estimation of lattice strain in nanometer-sized ZnO particles," *J. Theor. Appl. Phys.*, 6, 2–9, 2012, doi: 10.1186/2251-7235-6-6.

[19] P. M. Aneesh, K. A. Vanaja, and M. K. Jayaraj, "Synthesis of ZnO nanoparticles by hydrothermal method," *Nanophotonic Mater. IV*, 6639, 663901, 2014, 2007, doi: 10.1117/12.730364.

[20] R. C. De Souza, L. U. Haberbeck, H. G. Riella, D. H. B. Ribeiro, and B. A. M. Carciofı, "Antibacterial activity of zinc oxide nanoparticles synthesized by solochemical process," *Brazilian J. Chem. Eng.*, 36, 885–893, 2019, doi: 10.1590/0104-6632.20190362s20180027.

[21] J. Singh, S. Kaur, G. Kaur, S. Basu, and M. Rawat, "Biogenic ZnO nanoparticles: A study of blueshift of optical band gap and photocatalytic degradation of reactive yellow 186 dye under direct sunlight," *Green Process. Synth.*, 8, 272–280, 2019, doi: 10.1515/gps-2018-0084.

[22] A. K. Zak, M. E. Abrishami, W. H. A. Majid, R. Yousefı, and S. M. Hosseini, "Effects of annealing temperature on some structural and optical properties of ZnO nanoparticles prepared by a modified sol-gel combustion method," *Ceram. Int.*, 37, 393–398, 2011, doi: 10.1016/j.ceramint.2010.08.017.

[23] E. J. Ibrahem, Y. S. Yasin, and O. K. Jasim, "Antibacterial Activity of Zinc Oxide Nanoparticles Against Staphylococcus Aureus and Pseudomonas Aeruginosa Isolated from Burn Wound Infections," *Cihan Univ. Sci. J.*, 2017, Special-2, 265–277, 2017, doi: 10.24086/cuesj.si.2017.n2a24.

[24] E. Solati, L. Dejam, and D. Dorranian, "Effect of laser pulse energy and wavelength on the structure, morphology and optical properties of ZnO nanoparticles," *Opt. Laser Technol.*, 58, 26–32, 2014, doi:

10.1016/j.optlastec.2013.10.031.

[25] R. K. Dutta, B. P. Nenavathu, M. K. Gangishetty, and A. V. R. Reddy, “Studies on antibacterial activity of ZnO nanoparticles by ROS induced lipid peroxidation,” *Colloids Surfaces B Biointerfaces*, 94, 143–150, 2012, doi: 10.1016/j.colsurfb.2012.01.046.

[26] L. Nase *et al.*, “Effect of Long-Term Consumption of a Probiotic Bacterium, Lactobacillus rhamnosus GG, in Milk on Dental Caries and Caries Risk in Children,” *Caries Res.*, 35, 412–420, 2001, doi: 10.1159/000047484.

[27] S. Muthukumaran and R. Gopalakrishnan, “Structural, FTIR and photoluminescence studies of Cu doped ZnO nanopowders by co-precipitation method,” *Opt. Mater. (Amst).*, 34, 1946–1953, 2012, doi: 10.1016/j.optmat.2012.06.004.581–589.

[28] S. I. Al-Nassar, F. I. Hussein, and A. K. Ma, “The effect of laser pulse energy on ZnO nanoparticles formation by liquid phase pulsed laser ablation,” *J. Mater. Res. Technol.*, 8, 4026–4031, 2019, doi: 10.1016/j.jmrt.2019.07.012.

[29] S. Muthukumaran and R. Gopalakrishnan, “Structural, FTIR and photoluminescence studies of Cu doped ZnO nanopowders by co-precipitation method,” *Opt. Mater. (Amst).*, 34, 1946–1953, 2012, doi: 10.1016/j.optmat.2012.06.004.

[30] S. Matsuya, T. Maeda, and M. Ohta, “IR and NMR analyses of hardening and maturation of glass-ionomer cement,” *J. Dent. Res.*, 75, 1920–1927, 1996, doi: 10.1177/00220345960750120201.

[31] G. Szozda, K. Nowakowska, and D. Pawluch, “Comparative evaluation of the antibacterial activity of nitrofuran derivatives,” *Pol. Tyg. Lek.*, 42, 967–969, 1987.

[32] V. Svetlichnyi, A. Shabalina, I. Lapin, D. Goncharova, and A. Nemoykina, “ZnO nanoparticles obtained by pulsed laser ablation and their composite with cotton fabric: Preparation and study of antibacterial activity,” *Appl. Surf. Sci.*, 372, 20–29, 2016, doi: 10.1016/j.apsusc.2016.03.043.

[33] S. Talam, S. R. Karumuri, and N. Gunnam, “Synthesis, Characterization, and Spectroscopic Properties of ZnO Nanoparticles,” *ISRN Nanotechnol.*, 2012, 1–6, 2012, doi: 10.5402/2012/372505.

[34] R. A. Ismail, A. K. Ali, M. M. Ismail, and K. I. Hassoon, “Preparation and characterization of colloidal ZnO nanoparticles using nanosecond laser ablation in water,” *Appl. Nanosci.*, 1, 45–49, 2011, doi: 10.1007/s13204-011-0006-3.

[35]A. K. Zak, M. E. Abrishami, W. H. A. Majid, R. Yousefi, and S. M. Hosseini, “Effects of annealing temperature on some structural and optical properties of ZnO nanoparticles prepared by a modified sol-gel combustion method,” *Ceram. Int.*, 37, 393–398, 2011, doi: 10.1016/j.ceramint.2010.08.017.

[36] S. Yılmaz, E. O. Calikoglu, and Z. Kosan, “for an Uncommon Neurosurgical Emergency in a Developing Country,” *Niger. J. Clin. Pract.*, 22, 1070–1077, 2019, doi: 10.4103/njcp.njcp.

[37] H. H. Rashed, “Laser Pulses Effect on the Structural and Optical Properties of ZnO Nan particles Prepared by Laser Ablation in Water,” 3, 198–207, 2013.

[38] M. Gupta, R. S. Tomar, S. Kaushik, R. K. Mishra, and D. Sharma, “Effective antimicrobial activity of green ZnO nano particles of Catharanthus roseus,” *Front. Microbiol.*, 9, 1–13, 2018, doi: 10.3389/fmicb.2018.02030.

[39] P. Panpisut, N. Monmaturapoj, A. Srion, A. Toneluck, and P. Phantumvanit, “Physical properties of glass ionomer cement containing pre-reacted spherical glass fillers,” *Braz. Dent. J.*, 31, 445–452, 2020, doi: 10.1590/0103-6440202003276.

Tables

Table1: FTIR bonds of ZnONPs and ZnONPs-GI restorations samples.

Bond	**Wave number (cm^{-1})**		
	S1(100)	**S2(150)**	**S3(200)**
O-H bond	3312.42	3232.20	3231.20
ZnO	1633.71	1632.35	1631.35
C-H	526.72	493.78	530.40
	Sg1	**Sg2**	**Sg3**
C=O stretch	3722.39	3734.83	3937.39
GI	1639.49	1647.34	1657.23
C-H	422	532	995

Table2: The particle size and lattice strain of ZnONPs

Sample\Pulses	**Particle size (nm)**	**Lattice strain**
S1(100)	31.31	1.91
S2(150)	35.98	0.83
S3(200)	37.34	0.41

Table 3: Listed the Average diameter of ZnONPs and ZnONPs –GI restoration.

Average diameter(um)	Sample
31.3	S1
29.6	S2
27.2	S3
30.74	SG1
29.2	SG2
27.1	SG3

Figures

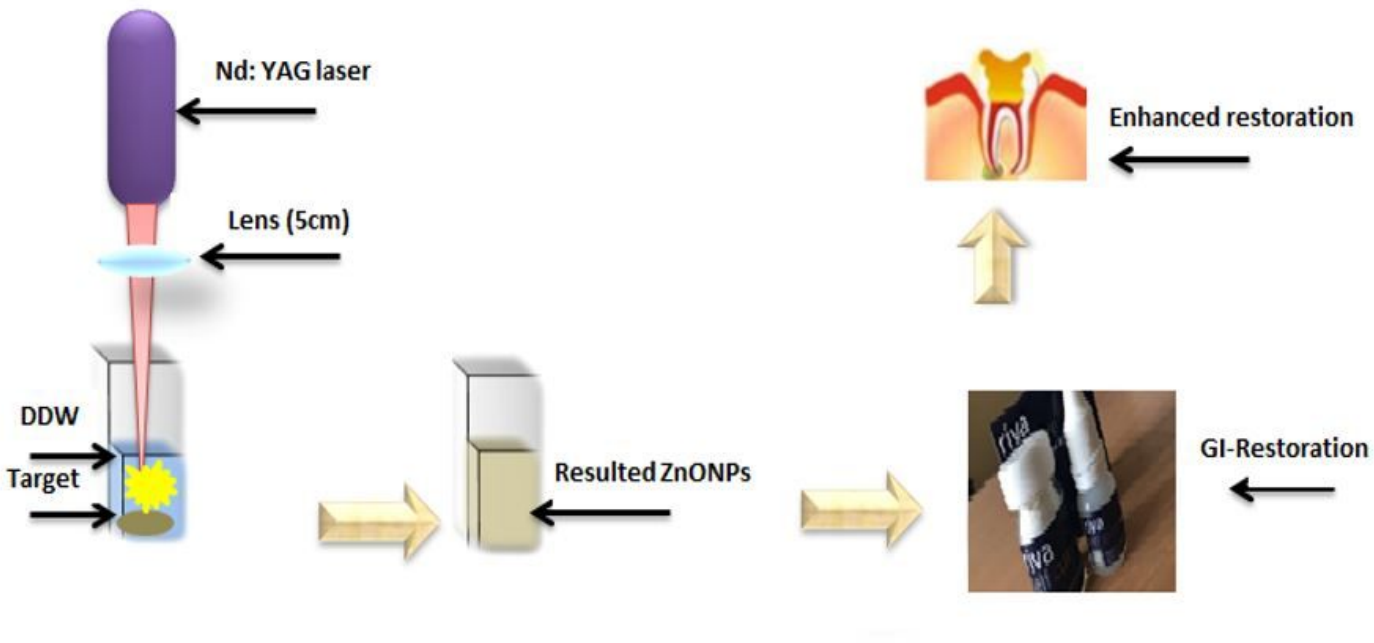

Figure 1

The experimental setup of preparation the enhanced restoration (ZnONPs +GI).

Figure 2

The tooth filled with enhanced restoration.

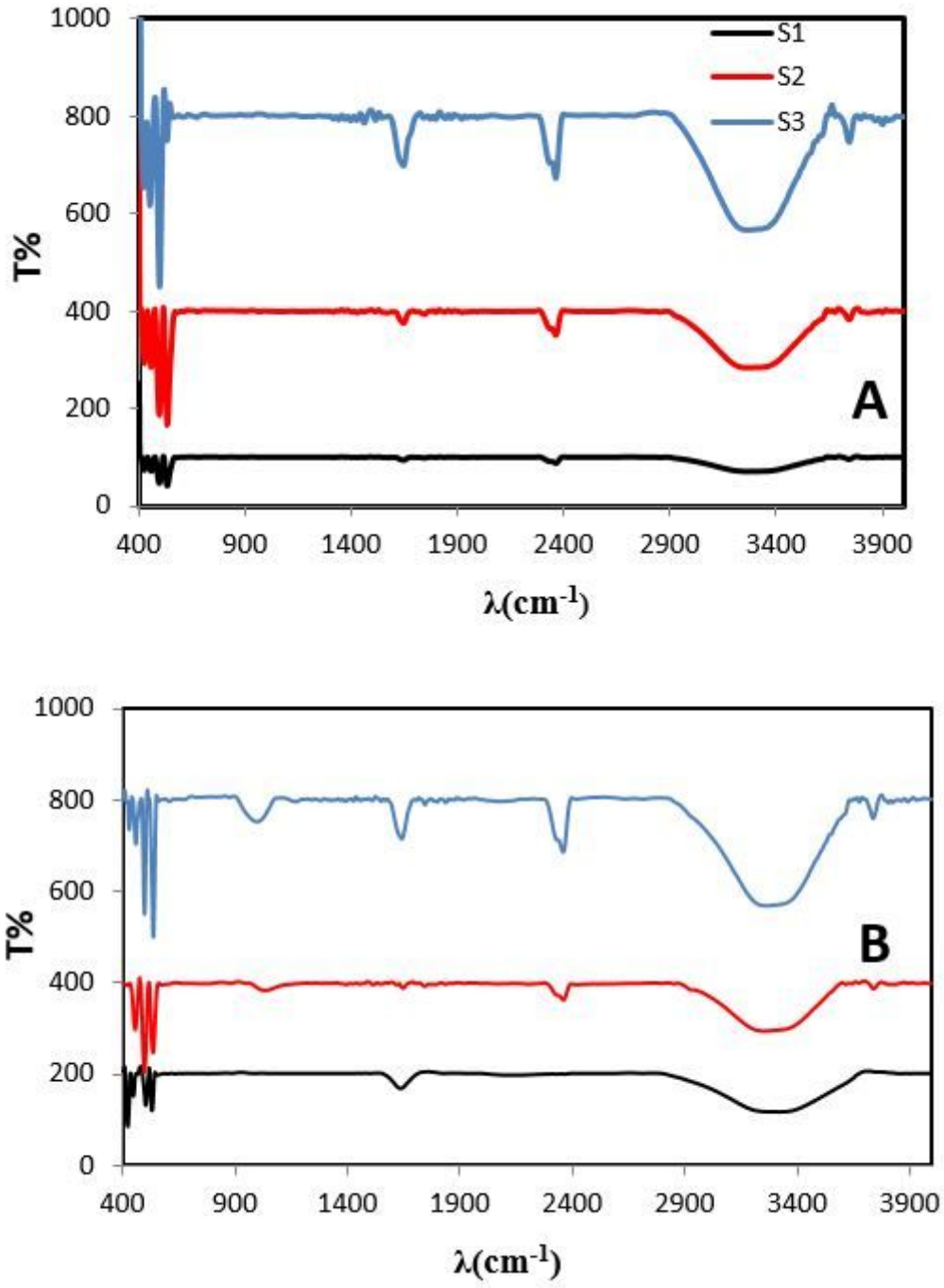

Figure 3

FTIR spectra of (A) Zinc oxide nanoparticles at different pulses and (B) ZnONPs-GI restoration.

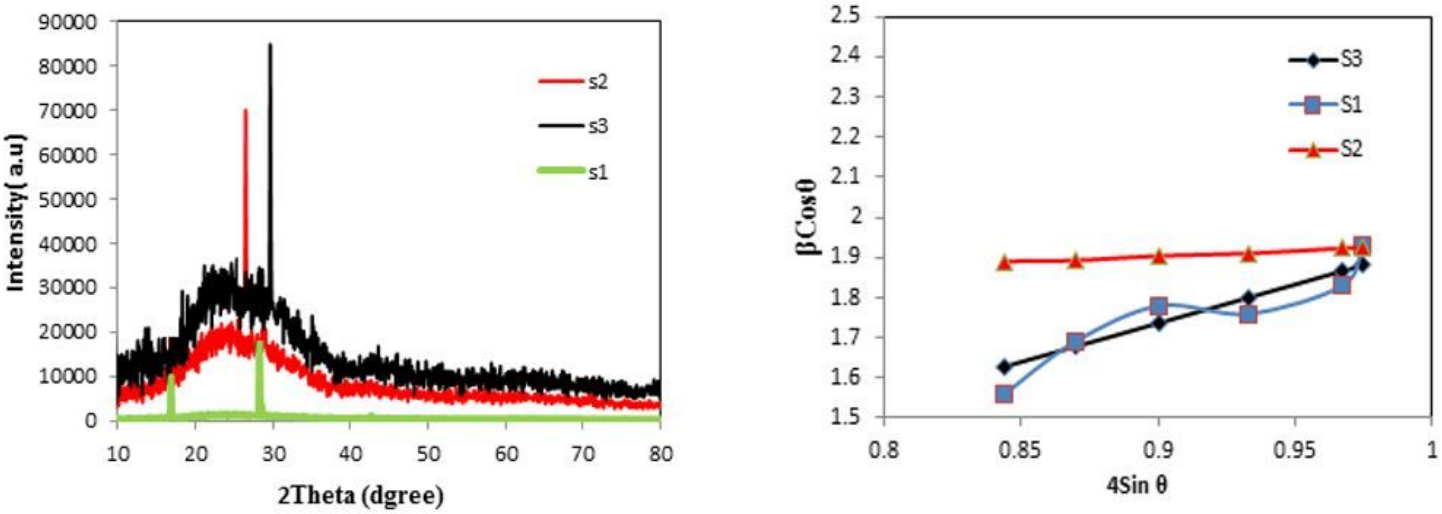

Figure 4

XRD patterns and strain extracted from the slope for ZnONPs colloidal

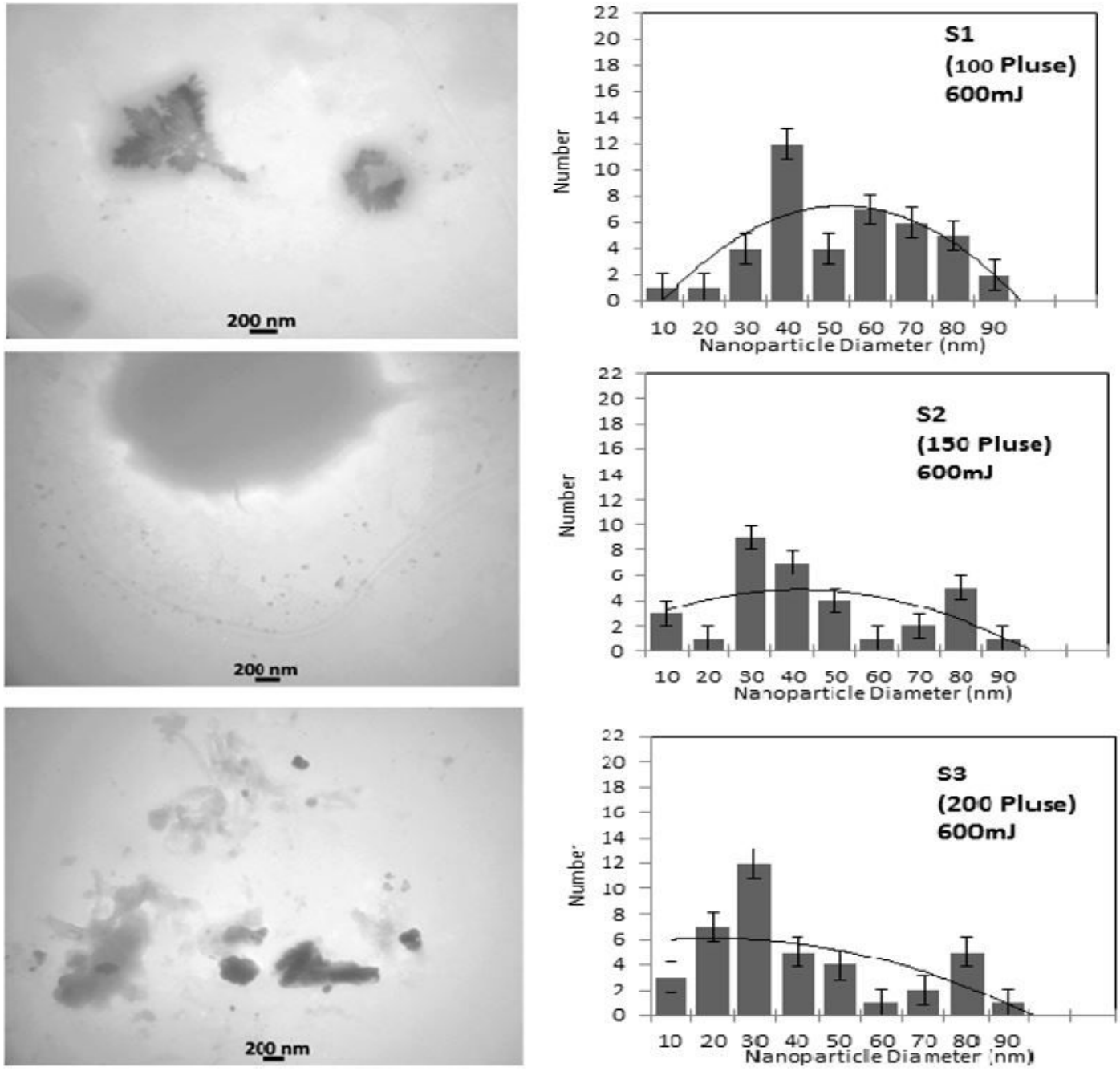

Figure 5

TEM image for ZnONPs prepared at different pulses with size distribution

Figure 6

Representative three dimensional high resolution atomic force microscopy images of the ZnONPs (S) samples and ZnONPs-GI (SG) restoration.

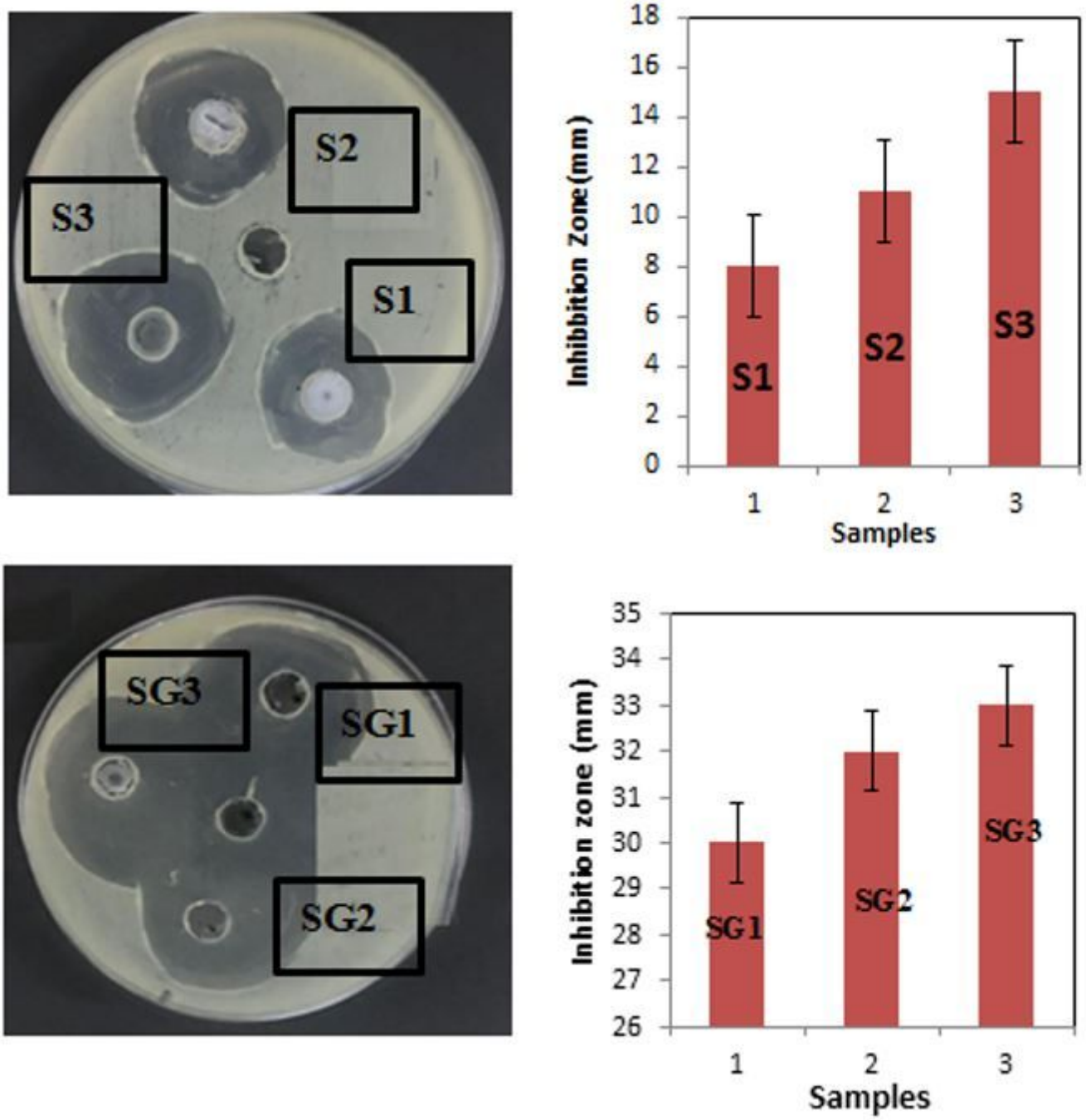

Figure 7

The antibacterial effect and inhibition zone for ZnONPs (S)and ZnONPs-GI(SG) restoration.

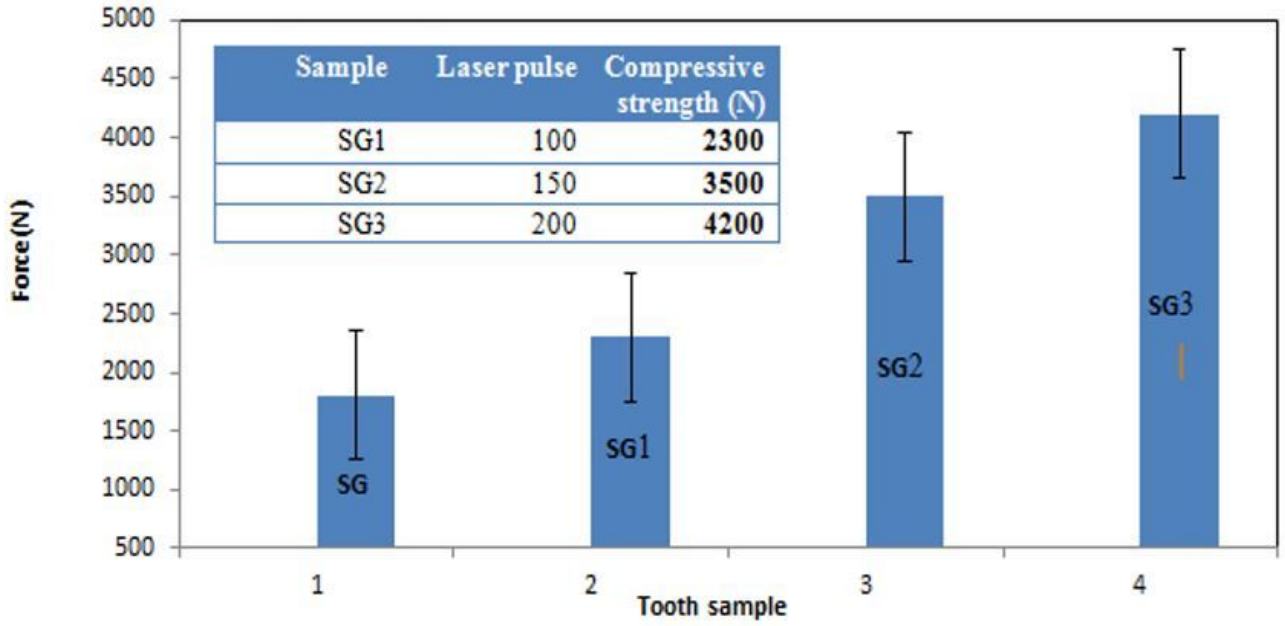

Figure 8

The compressive strength of tooth samples filled with enhanced restoration (ZnONPs-GI).